Huang, Haibing; Lv, Jun; Bao, Yameng; Xuan, Rongwei; Sun, Shenghua; Sneck, Sami; Li, Shuo; Modanese, Chiara; Savin, Hele; Wang, Aihua; Zhao, Jianhua

Data of ALD Al_2O_3 rear surface passivation, Al_2O_3 PERC cell performance, and cell efficiency loss mechanisms of Al_2O_3 PERC cell

Published in:
Data in Brief

DOI:
10.1016/j.dib.2016.12.030

Published: 01/04/2017

Document Version
Publisher's PDF, also known as Version of record

Please cite the original version:
Huang, H., Lv, J., Bao, Y., Xuan, R., Sun, S., Sneck, S., Li, S., Modanese, C., Savin, H., Wang, A., & Zhao, J. (2017). Data of ALD Al_2O_3 rear surface passivation, Al_2O_3 PERC cell performance, and cell efficiency loss mechanisms of Al_2O_3 PERC cell. *Data in Brief*, *11*, 19-26. https://doi.org/10.1016/j.dib.2016.12.030

Data in Brief 11 (2017) 19–26

Contents lists available at ScienceDirect

Data in Brief

journal homepage: www.elsevier.com/locate/dib

Data Article

Data of ALD Al_2O_3 rear surface passivation, Al_2O_3 PERC cell performance, and cell efficiency loss mechanisms of Al_2O_3 PERC cell

Haibing Huang [a,b,*], Jun Lv [a], Yameng Bao [b], Rongwei Xuan [a], Shenghua Sun [a], Sami Sneck [c], Shuo Li [b], Chiara Modanese [b], Hele Savin [b], Aihua Wang [a], Jianhua Zhao [a]

[a] *China Sunergy, No.123. Focheng West Road, Jiangning Zone, Nanjing, Jiangsu 211100, China*
[b] *Aalto University, Department of Micro and Nanosciences, Tietotie 3, Espoo 02150, Finland*
[c] *Beneq Oy, P.O. Box 262, Vantaa 01511 , Finland*

A R T I C L E   I N F O

Article history:
Received 21 November 2016
Received in revised form
13 December 2016
Accepted 15 December 2016
Available online 21 December 2016

A B S T R A C T

This data article is related to the recently published article ‘20.8% industrial PERC solar cell: ALD Al_2O_3 rear surface passivation, efficiency loss mechanisms analysis and roadmap to 24%’ (Huang et al., 2017) [1]. This paper is about passivated emitter and rear cell (PERC) structures and it describes the quality of the Al_2O_3 rear-surface passivation layer deposited by atomic layer deposition (ALD), in relation to the processing parameters (e.g. pre-clean treatment, deposition temperature, growth per cycle, and film thickness) and to the cell efficiency loss mechanisms. This dataset is made public in order to contribute to the limited available public data on industrial PERC cells, to be used by other researchers.

DOI of original article: http://dx.doi.org/10.1016/j.solmat.2016.11.018

* Corresponding author at: China Sunergy, No.123. Focheng West Road, Jiangning Zone, Nanjing, Jiangsu 211100, China.
E-mail address: haibing.huang@chinasunergy.com (H. Huang).

http://dx.doi.org/10.1016/j.dib.2016.12.030

Specifications Table

Subject area	Physics
More specific subject area	Silicon solar cells, device simulations
Type of data	Figures, tables, graphs, spectra
How data was acquired	Effective minority carrier lifetime, implied V_{oc}, pseudo I-V and illumination-V_{oc} curves by Sinton WCT-120 Suns-V_{oc} tester [2]; I-V curves and cell performances of the Si solar cell by HALM I-V tester or at Fraunhofer ISE; Thickness and refractive index of dielectric films by Suntech ellipsometer; Fixed negative charges (Q_f) and interface defect density (D_{it}) by Semilab SDI PV2000 [3]; Cross-sectional EDS analysis with Vantage-100 EDS instrument from Thermo Electron Corporation; Silicon solar cell series resistance components calculated using Meier's method[4]; Resistance in the sub-cell array measured by grid resistance tester; Contact resistance measured by grid resistance tester based on the transmission line model [5].
Data format	Raw and analyzed
Experimental factors	The wafer samples for lifetime, film thickness, refractive index, Q_f, and D_{it} were treated in NaOH solution to remove saw damage and cleaned in HCl and HF before the ALD Al_2O_3 process. PERC cells were processed from B-doped, Czochralski-grown, pseudo-square, 6″ wafers with 190 μm thickness. The processing flow is: saw damage removal (NaOH) with random-pyramid texturing, $POCl_3$ diffusion (front n^+ emitter, 90 Ω/□ sheet resistance), edge isolation with rear side polishing (HNO_3–HF–H_2SO_4 solution), ALD Al_2O_3 and PECVD SiN_x rear side passivation stacks, local patterning with laser ablation (532 nm, ps-laser), screen printing and co-firing for front (Ag/n^+–Si ohmic contact) and rear side metallization (Al local back surface field and local Al/p^+–Si Ohmic contact). For cell measurements, the completed solar cells were tested before light-induced degradation after storage in a nitrogen gas cabinet. Cross-sectional SEM/EDS analysis on the local Al–Si rear contact areas was done on three cross sections along the (110) crystallographic orientation with an angle of 45° with respect to the local line contacts at the rear.
Experimental features	The focus is on ozone (O_3) and $Al(CH_3)_3$ trimethylaluminium (TMA) based thermal ALD process, implemented by Beneq's industrial P800 batch ALD tool. Temperature is 200 °C, Al_2O_3/SiN_x thickness ratio is 10 nm/100 nm, deposition pressure is 150–500 Pa, rapid thermal processing (RTP) firing is at 760 °C peak temperature in compressed air for 2–3 s. The effective minority carrier lifetime and implied V_{oc} measurements were carried out with the generalized mode, $5 \cdot 10^{15}$ cm^{-3} injection level and optical constant of 0.7 for Si (100) surfaces and 0.85–0.95 for Al_2O_3/SiN_x stack. ALD Al_2O_3 process pressure and post-ALD anneal temperature and time were monitored by the process tool.
Data source location	(1) China Sunergy, No.123. Focheng West Road, Jiangning Zone, Nanjing, Jiangsu, 211100, China (2) Aalto University, Department of Micro and Nanosciences, Tietotie 3, 02150 Espoo, Finland
Data accessibility	Data is within this article and in Ref. [1]

Value of the data

- The data on the quality of the atomic layer deposition (ALD) Al_2O_3 rear surface passivation and on front Ag metallization pattern design provides a valuable dataset on the current industrial PERC structure and potentials, which can be used by researchers for the optimization of the current cell processes.
- The interplay between different parameters provides an overall description of the Al_2O_3 rear surface passivation process which leads to the optimal final passivation quality.
- The analysis on the loss mechanisms gives a relevant indication of the relative importance of different processing parameters via the calculation of the series resistance for the various components of the PERC cell.
- The data presented is collected from an extensive database from industrial PERC cells, and can thus be used by other researchers as a benchmark for industrial performances.

1. Data

The dataset of this paper provides additional information to Ref. [1]. The rear surface passivation quality in relation to the ALD Al_2O_3 processing parameters is reported in Figs. 1–5, the PERC cell properties are reported in Figs. 6–8 and Table 1, and the metal contact design pattern and parameters are reported in Table 2.

2. Experimental design, materials and methods

The procedure prior to the minority carrier lifetime measurements on the ALD Al_2O_3 rear surface passivation is described in detail in Fig. 1 in Ref. [1] and the most relevant aspects are reported here. All samples underwent saw damage removal and pre-ALD clean, followed by ALD Al_2O_3 deposition with varying parameters. Post-ALD anneal was performed on most of the samples, and then followed by plasma enhanced chemical vapor deposition (PECVD) of the SiN_x capping layer. Afterwards, since lifetime cannot be measured after metallization, the samples were divided into two groups; one group directly underwent rapid thermal processing (RTP) firing, whereas a second group first underwent screen-printing of Al paste, then RTP firing followed by Al paste removal. All the samples were then measured under similar parameters.

The interface defect density (D_{it}), the negative fixed charges (Q_f) and open circuit voltage (V_{oc}) as a function of the pre-ALD clean parameters are reported in Fig. 1. SC1 and SC2 pre-clean can achieve the best passivation quality (both regarding D_{it} and V_{oc}). The pre-ALD clean does not affect the amount of Q_f. Note that in the industrial PERC cell process, edge isolation and rear side polishing prior to the Al_2O_3 process normally terminate with HCl–HF clean sub-step.

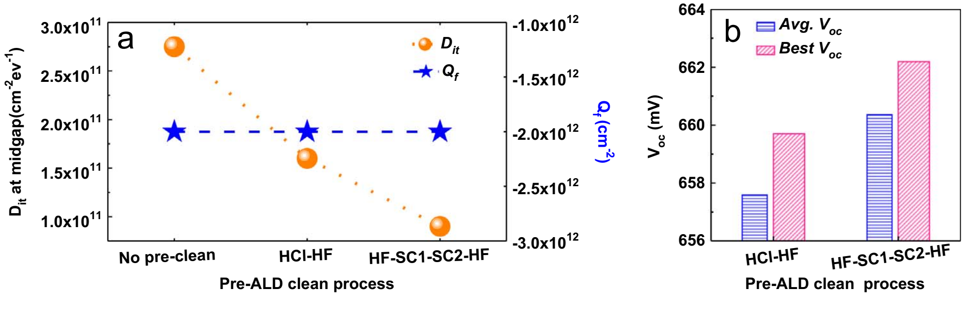

Fig. 1. D_{it} and Q_f (a) and V_{oc} (b) as a function of pre-ALD clean for Al_2O_3 passivation.

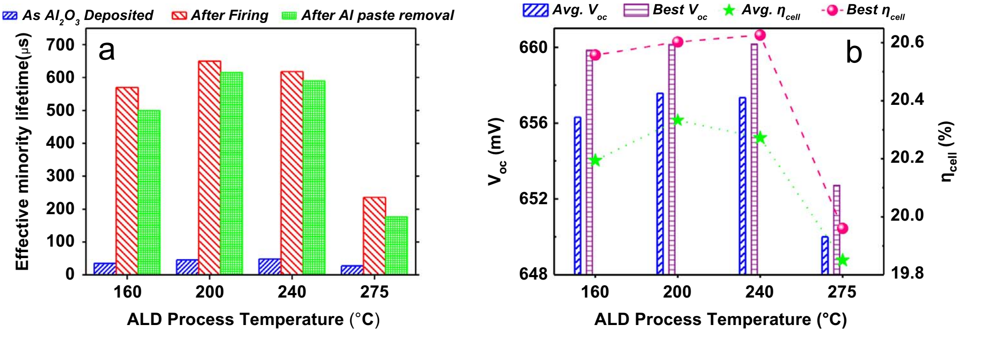

Fig. 2. Effective minority carrier lifetime (a) and cell performance (b) as a function of ALD temperature for Al_2O_3 passivation.

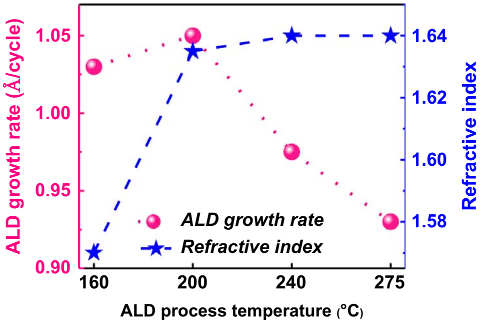

Fig. 3. Growth rate (Å/cycle) and refractive index as a function of ALD process temperature.

The effect of the ALD process temperature for Al_2O_3 passivation on effective minority carrier lifetime and PERC cell performance (as V_{oc} and cell efficiency (η_{cell})) is reported in Fig. 2, while the effect on growth rate and refractive index (n_k) of the dielectric layer is shown in Fig. 3. Our data show that the optimal temperature for passivation (in relation to both the effective lifetime and η_{cell}) is in the range of 200–240 °C, whereas the passivation level drops sharply at 275 °C. Note also that the process window between 160 and 240 °C is broad. In addition, the growth rate begins to decrease for temperatures above 200 °C. The refractive index is relatively low below 200 °C (n_k=1.57), and it is stable (n_k=1.63–1.65) between 200 and 400 °C. The optimal temperature for growth rate and refractive index is also around 200 °C.

Fig. 4 shows the passivation quality as effective minority carrier lifetime, PERC cell performance (V_{oc} and η_{cell}), D_{it} and Q_f as a function of the Al_2O_3 film thickness. Effective minority lifetime and cell performance gradually increase with thickness increasing from 3.5 to 16 nm, where the optimal thickness is ~10 nm. When the film thickness increases from 3.5 to 16 nm, cell performances and D_{it} gradually improve, while Q_f is at the same level. Note that even a thin Al_2O_3 film of about 3.5 nm can work well on PERC cell ($V_{oc} \approx 652$ mV and $\eta_{cell} \approx 20.3\%$).

SEM/energy dispersive X-ray spectroscopy (EDS) analysis on the effect of voids on the local back surface field (LBSF) rear local contact was performed and is shown in Fig. 5. Note that the spectra in the figure are from the Al-Si eutectic, the Al LBSF and the Si substrate, respectively. The detailed interpretation of the differences among the spectra is given in Ref. [1]. The thickness of the Al LBSF layer is ~10 μm, thus revealing that the junction depth is deeper than 10 μm.

Representative examples of industrial PERC cell performances are reported in Figs. 6,7. The certified current-voltage (I-V) curve and cell performance of one SiO_2-PERC cell was measured at

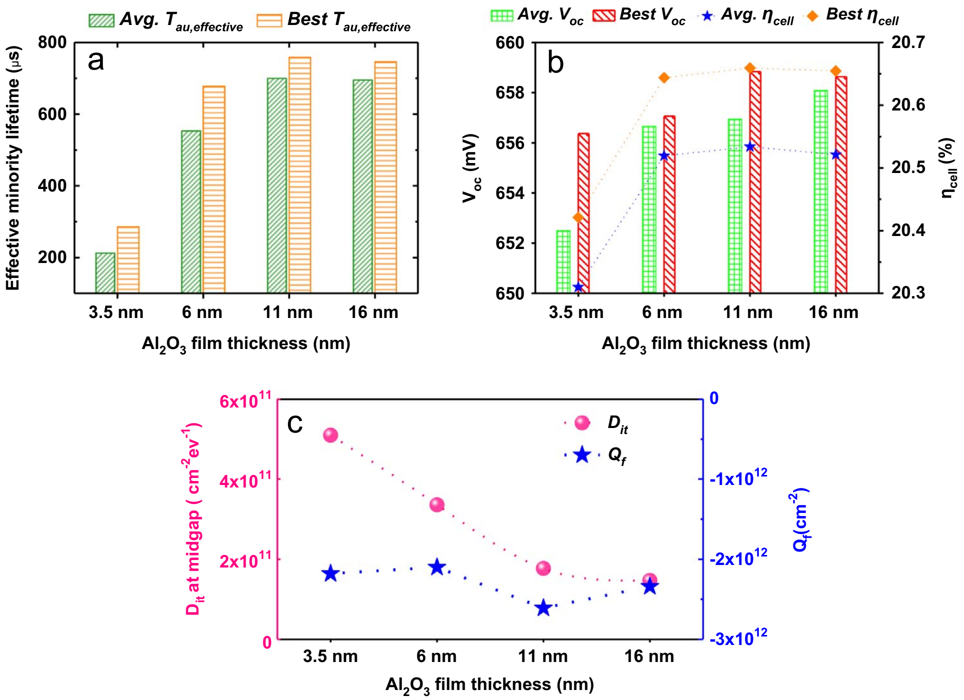

Fig. 4. Effective minority carrier lifetime (a), V_{oc} and η_{cell} (b), D_{it} and Q_f (c) as a function of Al_2O_3 film thickness for Al_2O_3 passivation.

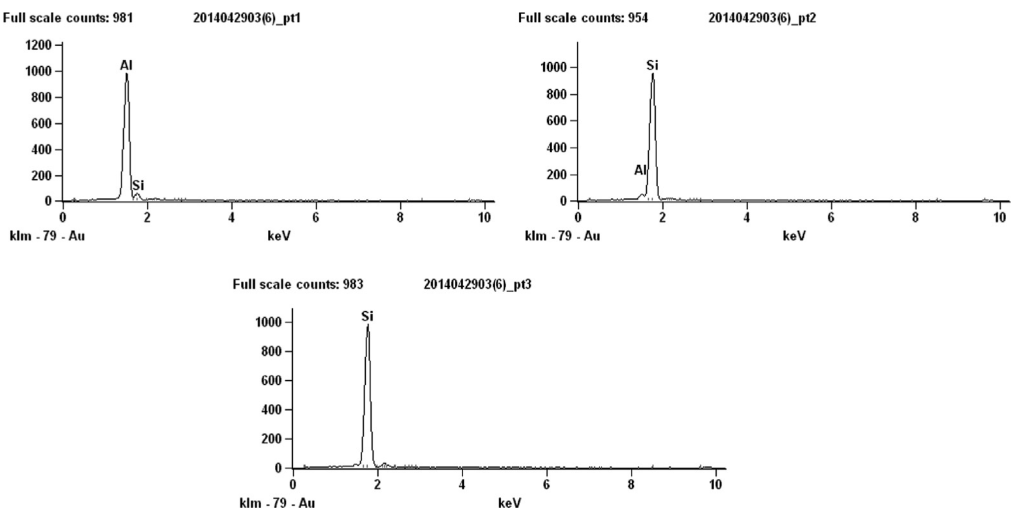

Fig. 5. Cross-sectional EDS analysis of the Al-Si contact areas (Fig. 14-c and Table 4 in Ref. [1]). Here, point 1 (pt1): Al-Si alloy, point 2 (pt2): Al LBSF, and point 3 (pt3): Si substrate.

Fraunhofer ISE in July 2013 under standard test conditions (see Fig. 6). Note that the key process in this structure is rear surface passivation with thermal oxidation and dielectric opening with Merck's chemical paste. Fig. 7 shows a typical example of the cell efficiency of an average

Mismatch factor : (for spectral correction)	=	0.9892	
Area (t)[1]:	=	239.62	cm²

IV-curve parameter under standard testing conditions (STC):

V_{OC}	=	662.8	mV
I_{SC} (Ed.2 - 2008)	=	9.40	A
J_{sc}	=	39.24	mA/cm²
I_{MPP}	=	8.79	A
V_{MPP}	=	552.2	mV
P_{MPP}	=	4.855	W
FF	=	77.91	%
η	=	20.26	%

For comparison purposes:
Calculated value according to previous standard spectrum:
I_{SC} (Ed.1 - 1989) = 9.33 A

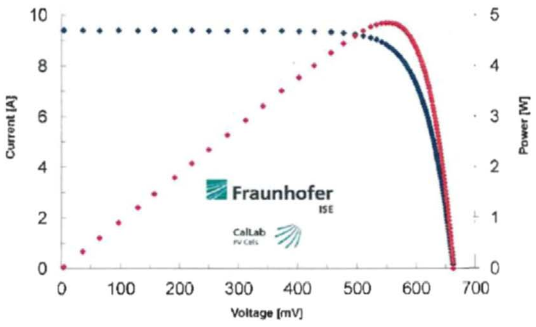

Fig. 6. Cell performance and I-V curve of one SiO_2-PERC cell example (before light induced degradation) tested by Fraunhofer ISE in July 2013 (under Standard Test Condition of global AM1.5, 1000 W m^{-2}, 25 °C).

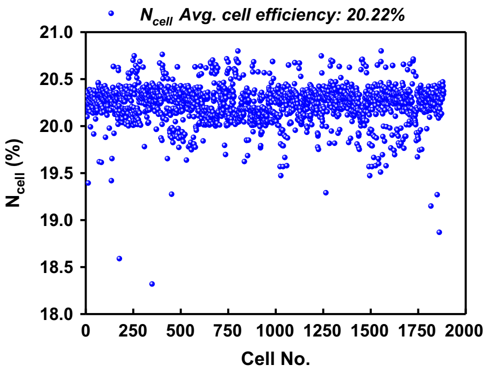

Fig. 7. The scatter diagram of the industrial Al_2O_3 PERC cell performance (~2000 PERC cells/batch, before light induced degradation).

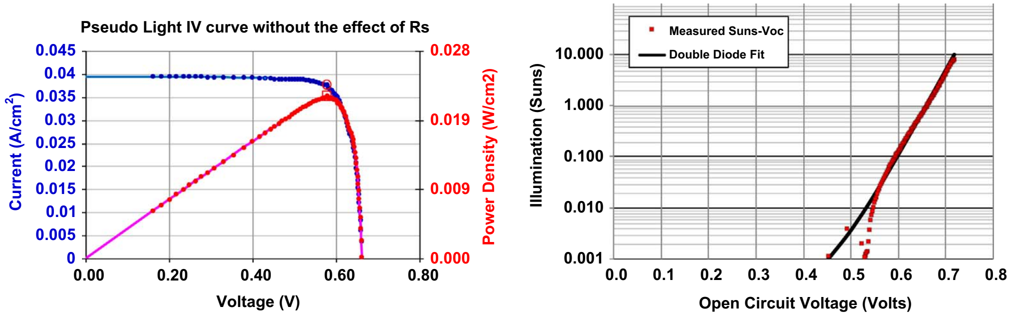

Fig. 8. Suns-V_{oc} measurement of the PERC cell sample A (Table 5 in Ref. [1]): pseudo I-V curve (left) and illumination-V_{oc} (right).

Table 1
The calculation of series resistance of the industrial Al_2O_3 PERC cell using Meier's method [4].

Description	Key measurement		Specific resistance (Ω cm^2)	resistance (mΩ)	Fraction
	Item	Measured value			
1. Front Ag busbar	Resistance length of busbar	0.098	0.0073	0.0299	1.22%
2. Rear AgAl busbar	Similar to front busbar	estimated	0.0040	0.0165	0.67%
3. Front Ag grid	Busbar-to-busbar resistance	0.055 Ω	0.2197	0.9070	36.82%
4. Rear Al metallization	R_{sheet_metal}	0.009 Ω/□	0.0419	0.1730	7.02%
5. Front n^+ emitter	$R_{sheet\_emitter}$	90 Ω/□	0.1971	0.8137	33.03%
6. Rear Si substrate lateral spreading resistance	$R_{sheet\_Si\ substrate}$	121 Ω/□	0.0746	0.3081	12.51%
7. Front Ag/n–Si contact	TLM measurement [5]	Specific contact resistance: 3.1 mΩ cm^2	0.0161	0.0665	2.70%
8. Rear Al/p–Si contact	TLM measurement [5]	Specific contact resistance, estimated	0.0030	0.0124	0.50%
9. p–Si substrate	Resistivity, thickness of wafer	2 Ω cm, 165 μm	0.0330	0.1362	5.53%
R_s-Total	–	–	0.5967	2.4635	100%

Table 2
The basic information of the design pattern of the front Ag contact of the Al_2O_3 industrial PERC cell in this data article.

Key parameters	Description	Value
n-front Ag	the number of front grid	96
b-front Ag	half of the length between each adjacent front Ag grid	0.081 cm
Front Ag finger	width/height	50 μm/20 μm
n-rear Al	180, line array	~30 μm
b-rear Al	half of the length between each adjacent rear Al line	0.043 cm
Front busbar (5 busbar)	busbar width	0.08 cm
Front Ag metal fraction	–	5.65%
Rear Al metal fraction	–	3.25%

industrial batch of China Sunergy's Al_2O_3 PERC cell, tested in house under standard conditions (i.e., the same I-V test criteria used as Fraunhofer ISE).

An example of a representative Al_2O_3 PERC cell (sample A) measured by illumination-V_{oc} is shown in Fig. 8, where the sample was tested before light-induced degradation (LID).

The series resistance (R_s) of the industrial Al_2O_3 PERC cell is shown in Table 1, calculated according to Meier's method [4]. This calculation method is based on the measurement of R_s components in a sub-cell (the measurement array), shown as key measurement in Table 1. The resistance in the different regions of the sub-cell array was measured by the grid resistance tester, while the specific contact resistance was measured by the grid resistance tester based on the transmission line model (TLM) method [5]. In addition, Table 2 provides the basic information of the design pattern of the front Ag contact, which can support the calculation of Table 1. The detailed interpretation of the calculation results can be found in Ref. [1].

Acknowledgements

The research work is based on the China-Finland International R&D Cooperation project "Improved cost-efficiency in crystalline silicon solar cells through Atomic Layer Deposited Al_2O_3", Project No. 40843 (Chinese Project No. S2013GR0622), 2013.05-2016.05. The work has been partially funded through the European Research Council under the European Union's FP7 Programme ERC Grant Agreement No. 307315.

Transparency document. Supporting material

Transparency data associated with this paper can be found in the online version at http://dx.doi.org/10.1016/j.dib.2016.12.030.

References

[1] H. Huang, J. Lv, Y. Bao, R. Xuan, S. Sun, S. Sneck, S. Li, C. Modanese, H. Savin, A. Wang, J. Zhao, 20.8% industrial PERC solar cell: ALD Al_2O_3 rear surface passivation, efficiency loss mechanisms analysis and roadmap to 24%, Sol. Energy Mater. Sol. Cells 161 (2017) 14–30.
[2] R.A. Sinton, A. Cuevas, Contactless determination of current-voltage characteristics and minority-carrier lifetimes in semiconductors from quasi-steady-state photoconductance data, Appl. Phys. Lett. 69 (1996) 2510–2512.
[3] ⟨https://www.semilab.hu/products/si/faast-cocos-mc.https://www.semilab.hu/products/pvi/pv-2000⟩, 2016.
[4] D. Meier, E. Good, Determining components of series resistance from measurements on a finished cell, in: Proceedings of the 4th WCPEC, 2006, pp. 1315–1318.
[5] D.L. Meier, D.K. Schroder, Contact resistance: its measurement and relative importance to power loss in a solar cell, IEEE Trans. Electron Devices 31 (1984) 647–653.